Research article

Yuting Zhao[a], Shuaiwen Gan[a], Leiming Wu, Jiaqi Zhu, Yuanjiang Xiang and Xiaoyu Dai*

GeSe nanosheets modified surface plasmon resonance sensors for enhancing sensitivity

https://doi.org/10.1515/nanoph-2019-0170
Received June 10, 2019; revised August 5, 2019; accepted August 28, 2019

Abstract: Germanium selenide (GeSe) nanosheets are stable and inexpensive and considered to have a great potential for photovoltaic applications, however we have demonstrated that GeSe nanosheets are also promising for sensing technology, in this paper. By spin-coating the GeSe nanosheets on the surface of noble metal (Au), we have obtained a surface plasmon resonance (SPR) sensor with significantly enhanced sensitivity, and the performance of the sensor is closely related to the thickness of the GeSe film. By detecting different refractive index solutions, we have obtained the optimized sensitivity with 3581.2 nm/RIU (which is nearly 80% improvement compared to traditional SPR sensors) and figure of merit with 14.37 RIU^{-1}. Moreover, the proposed SPR sensor was vastly superior in sensing Pb^{2+} heavy metal ions after coating it with chitosan and GeSe composite. A maximum sensitivity of 30.38 nm/μg/l has been verified, which is nearly six times better than that of conventional SPR sensor. Our results demonstrated that GeSe nanosheets overlayer with modified SPR sensor has its great potential in heavy metal detection and chemical-specific molecular identification.

Keywords: germanium selenide; surface plasmon resonance sensor; sensitivity; Pb^{2+} heavy metal ions.

[a]**Yuting Zhao and Shuaiwen Gan:** These authors contributed equally to this work.
***Corresponding author: Xiaoyu Dai,** SZU-NUS Collaborative Innovation Center for Optoelectronic Science and Technology, Key Laboratory of Optoelectronic Devices and Systems of Ministry of Education and Guangdong Province, Institute of Microscale Optoelectronics (IMO), Shenzhen University, Shenzhen 518060, China, e-mail: xiaoyudai@126.com. https://orcid.org/0000-0002-0180-8357
Yuting Zhao, Shuaiwen Gan, Leiming Wu, Jiaqi Zhu and Yuanjiang Xiang: SZU-NUS Collaborative Innovation Center for Optoelectronic Science and Technology, Key Laboratory of Optoelectronic Devices and Systems of Ministry of Education and Guangdong Province, Institute of Microscale Optoelectronics (IMO), Shenzhen University, Shenzhen 518060, China

1 Introduction

In recent years, researches on sensing applications using some superior two-dimensional (2D) materials, such as graphene, black phosphorus (BP), and transition metal dichalcogenides (TMDCs), have gained widespread attention [1–3], because of their unique electronic and optical properties [4, 5]. In addition to these 2D materials, germanium selenide (GeSe), a novel layered semiconductor 2D material located in the fourth group, is also commonly applied in a range of important fields such as electronic devices, photodetectors, and sensor chips due to its strong absorption of visible light [6–8], high stability, and extremely narrow band gap [9]. 2D GeSe has both direct and indirect band gaps, and the direct band gap of a single GeSe layer is about 1.15 eV [10]. Based on the quantum confinement effect, it can be found that when the thickness of 2D GeSe increases continuously, its band gap gradually decreases, thus forming an electronic property depending on the thickness relationship of the material, resulting in an excellent anisotropic characteristic [11]. Therefore, it is attempted to apply few-layer of GeSe as sensing chip in sensing detection technology as the specific research of 2D GeSe in sensing technology is rare, which needs further exploration.

Surface plasmon resonance (SPR) is a collective vibration of free charge along the interface between the metal layer and dielectric under the excitation of incident light in transverse magnetic (TM) mode [12], and the condition of the resonance is that the wave vector of SPPs matches to that of the evanescent wave. SPR sensing technology offers significant advantages in detecting the interaction of tiny analytes by virtue of the small changes of the refractive index within the sensing layer surface [13, 14], including free labeling of analytes, real-time monitoring of the reaction state of analytes, and low cost [15]. Generally, SPR sensors are divided into two structures, Kretschmann and Otto configurations [16], while Kretschmann configuration is more widely used. The simplest Kretschmann configuration consists of a coupling prism, a metal film in the middle layer, and a sensing medium at the bottom, in which the metal film is selected according to the desired resonance in the reflection spectrum. A gold film is considered as the most suitable choice due to the strong antioxidant capacity, great optical properties and chemical stability [17]. However, the gold films still have a series of limitations, such as poor compatibility and adsorption of gold film with biomolecules [18], resulting in low detection sensitivity, especially for some traces of small molecular analytes with low concentration.

In order to solve the above problems that restricts the enhancement of sensor sensitivity, biomolecular recognition elements (BRE) covering the metal layer, graphene, topological insulator, and other 2D materials [19] are applied to enhance the bonding affinity of the detected analytes, which greatly improves the sensitivity of SPR sensors. In consequence, we have considered covering GeSe nanosheet on the gold film that is directly contacting the sensing interface analytes to more quickly sense the change of the refractive index of the contact area.

In this study, we have done the numerical simulation first and indicated that the GeSe film can enhance the sensitivity significantly. Then the outstanding sensing performance was discussed experimentally. First, we studied the effect of GeSe nanosheets' thickness on the sensitivity enhancement of SPR sensor, where the thickness of GeSe overlayer is controlled by spin-coating time of the GeSe nanosheets. The prepared structure was used to detect a series of solutions with different refractive indices. It was found that with the increase in GeSe thickness, the sensitivity of wavelength modulation can reach a maximum value of 3581.2 nm/RIU at four times spin-coating, which was near 80% higher than that of traditional SPR senor covered only with gold film. To clearly illustrate the superior performance of the proposed sensor with high sensitivity, we took advantage of it to detect the different concentration of lead ions (Pb^{2+}).

Excessive heavy metal ions cause serious health hazards to human such as affecting the functions of central nervous system, endocrine glands, immune system, and bones [20, 21]. According to International Medical Standards, the lead ion content in normal human blood should be less than 100 µg/l. The detection methods in tracing lead ions below this standard value usually include atomic absorption spectroscopy [22–24], inductively coupled plasma mass spectroscopy [25, 26], electrochemical impedance spectroscopy [27], and polarography [28]. However, due to the limitations of high cost, complicated sample preparation, and long detection time, we intended to detect lead ions with SPR sensor based on GeSe and chitosan mixture nanomaterial, in which chitosan is an abundant organic polymer with strong absorption capacity for heavy metals. The final results showed that the GeSe-chitosan SPR senor has a significant enhancement in detection sensitivity, spectral resolution and detection limit for lead ions comparing with traditional SPR sensors

2 Experiment

2.1 Materials and reagents

The concentration of GeSe alcohol aqueous solution (Nanjing, Muke Nano Technology Co., Ltd.) used in the experiment is 0.1 mg/ml and its nanosheet size is about 50–200 nm. Deacetylation was carried out by dissolving 0.40 g of chitin (Shanghai, Macklin) with medium molecular size into 50 ml of 1% acetic acid solution (Shanghai, Aladdin), followed by crosslinking modification with 0.05 g of glutaraldehyde (Shanghai, Sigma-Aldrich) to finally obtain a desired chitosan solution at room temperature. The lead ions standard solution with a concentration of 1 µg/l (Ruiqi, Shanghai) was continuously diluted to 0.2 µg/l, 0.4 µg/l, 0.6 µg/l, and 0.8 µg/l, respectively to obtain four different concentrations of diluted lead ions solution. An ethylene glycol solution (Shanghai, Aladdin) having RI of 1.333, 1.3384, 1.347, 1.3536, and 1.3605 was prepared by using an Abbe refractometer.

2.2 Preparation of sensor films and optical characterization instrument

BK7 Dove prism (Da Heng Optical-GCL-030602, China) with a refractive index of 1.5151 at the bottom of the Kretschmann structure was cleaned with acetone solution before the experiment, and the gold film (the thickness is near 50 nm) adhered to the extremely thin chromium (Cr, 5 nm) layer was firmly covered by matching liquid on the coupling prism. Then, a thin layer of GeSe and chitosan were formed on the surface of gold film by spin coating technique (Schwan technology, USA) at a spin speed of 600 rpm for one minute with approximately 0.6 ml of solution on the substrate. Before starting the experiment, the prepared sensor chip was allowed to stand at room temperature for three hours so that the aqueous alcohol solution was completely evaporated. In addition, the prepared solution was centrifuged with an ultrasonic instrument for half-an-hour to make the distribution more uniform. The Raman spectroscopy measurements were performed by using the Raman system (HORIBA JY LabRAM HR Evolution). The cross-section images of GeSe nanosheets were detected by scanning electronic microscope (Supra 55 Sapphire, Carl ZEISS, Germany).

2.3 SPR experimental set-up

The experimental optical path structure of the SPR sensor is shown in Figure 1. A multicolor wide beam is emitted from the Tungsten Halogen source (Ocean Optical-HL-2000, America) (wavelength ranging from 300 to 1000 nm) and formed into a focusing collimation transmission light with transverse magnetic (TM) mode through a polarizer and a focusing prism. Next, the incident beam from one side of BK7 prism is coupled with another prism to excite SPPs, and the reflected light on the other side is collected and analyzed by the spectrometer through optical fiber transmission (Ocean Optical-P200-2-UV-VIS, America). The experiment adopts a wavelength-interrogated sensing detection method. By dropping an appropriate amount of the analyte onto the surface of sensor chip, it is possible to clearly observe the apparent absorption peak of the obtained reflection spectrum. With the change of the RI in analyte, the position of the resonant wavelength also changes in which the wavelength shifts describe the sensitive performance of the sensor. All steps are carried out under laboratory conditions (temperature 22°C, humidity 50%).

3 Results and discussion

Before our experiment, we did the numerical simulation on the schematic diagram of Figure 1. In this structure, light enters the Dove prism horizontally, hence we calculated the incident angle $\theta = 45° + \sin^{-1}\left(\frac{\sin 45°}{n_{BK7}(\lambda)}\right)$ at the interface gold and Dove prism by Snell's law, where $n_{BK7}(\lambda)$ is the refractive index of BK7 prism. The optical constants of BK7 Dove prism, Cr, and Au can be obtained from the experimental measurement [29–31]. The optical constants of GeSe monolayer are given in references [32, 33]. For calculating the reflection intensity of the TM-polarized light of the configuration, we employed the N-layer transfer matrix method [34].

We defined the performance of the sensor by calculating several common parameters: sensitivity (S) and the figure of merit (FOM), with $S = \Delta\lambda/\Delta n$ and FOM = S/FWHM, where FWHM is the full width at half maximum. As shown in Figure 2A and B, the reflectance with respect to the wavelength for the conditions of only single Au film and Au-GeSe film when the refractive index of sensing medium (n_s) is 1.33, 1.34, 1.35 and 1.36, respectively. We can obtain the resonance wavelength shift from that and calculate the FWHM as 65 nm and 145 nm at $n_s = 1.33$. In Figure 2C, we plotted the fitting curve for the resonance wavelength with respect to the refractive index of sensing medium, the linear slope showing the sensitivity are 2560 nm/RIU for single Au film and 3450 nm/RIU for Au + GeSe structure, besides, the FOM are 39.38/RIU and 23.79/RIU, respectively. This indicates that the GeSe film can enhance the sensitivity significantly. Figure 2D plotted the electric field distribution of the TM polarized light (with the wavelength of 633 nm) of the proposed structure, $|E_0|$ represents the electric intensity in prism. The evanescent normalized electric intensity reached the maximum of 15.869, 18.187, 20.378 and 22.912 at the interface of GeSe and sensing medium for $n_s = 1.33$, 1.34, 1.35 and 1.36, respectively. This means GeSe film can improve the electric field intensity, as well as the

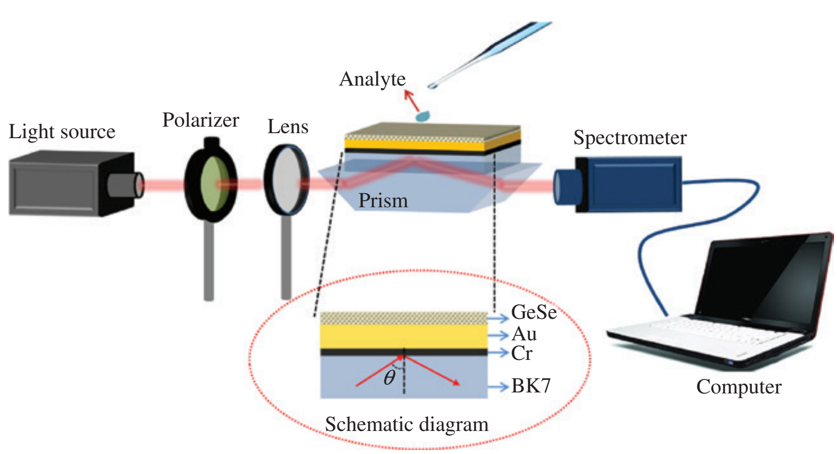

Figure 1: Experimental set-up for SPR sensor technique.

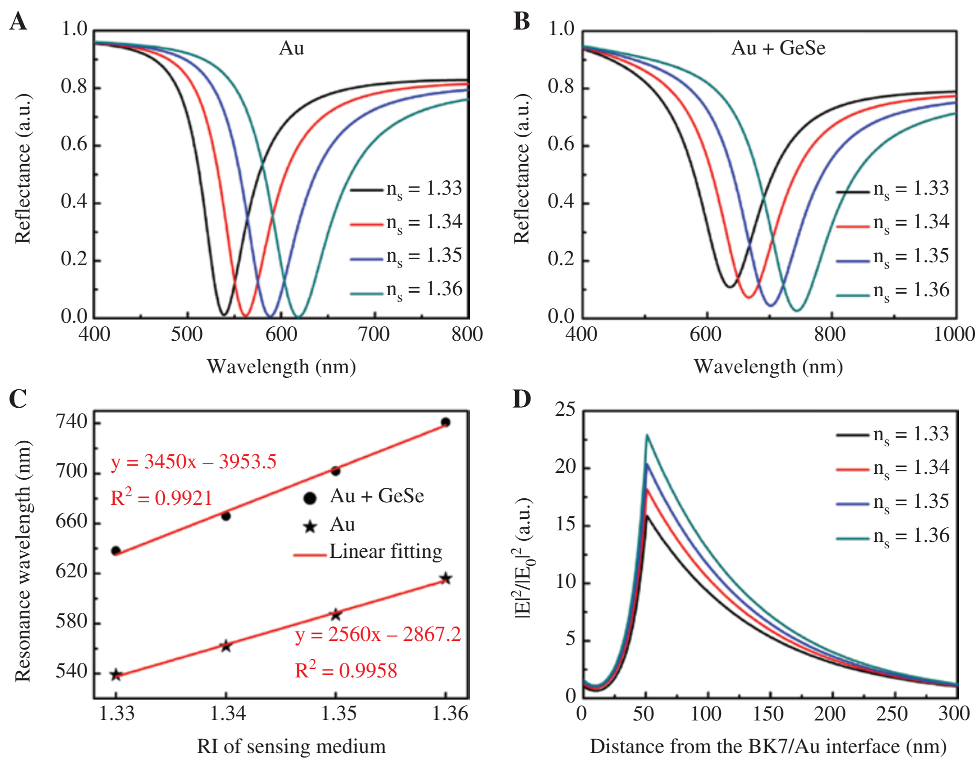

Figure 2: The numerical simulation results of the structure.
Numerical simulation of reflectance with respect to the wavelength for (A) the conventional condition with only single Au film and (B) the proposed structure with additional GeSe monolayer film. (C) Fitting curve for the resonance wavelength with respect to the refractive index of sensing medium, which show the sensitivity with 2560 nm/RIU for single Au film and 3450 nm/RIU for Au + GeSe structure. (D) The electric field distributions of the proposed structure with Au + GeSe film.

enhancement of the SPPs excitation [35]. Moreover, the evanescent electric field in the sensing medium decreases exponentially. Thanks to the maximum intensity at the interface of GeSe/sensing medium and the increase in the evanescent depth in the analyte medium will maximize the sensitivity of the sensor [36, 37].

To verify that GeSe film can enhance the performance of the SPR sensor, we have done related experiments.

Since the thickness of the layered GeSe nanosheets covered on the gold film is a variable for the optimization of the sensor performance, we achieved this goal by different number of spin coatings in the experiment. The Raman scattering spectrum of GeSe nanosheets is depicted in Figure 3 for describing structural estimations. The excitation source wavelength of the Raman microscope is 532 nm. The excitation peaks B_{3g} and A_g^3 of the two different modes correspond to 151 cm^{-1} and 188 cm^{-1}, respectively, which is consistent with previous studies [1, 33]. A scanning electron microscope (SEM) image of GeSe nanosheets overlying a gold film is presented in Figure 4, depicting the surface topography of the spin-coating layered material over the gold film and the GeSe thickness in the cross-sectional direction. According to the effect of

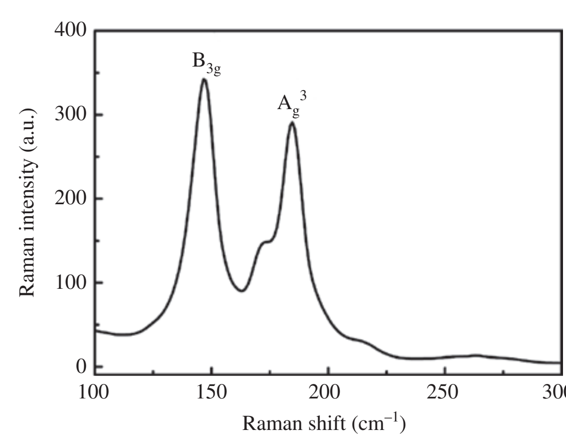

Figure 3: Raman spectrum of GeSe nanosheets.

the sensing performance enhancement during the experiment, GeSe was repeatedly spin-coated for five times, and the uniform thicknesses of the cross section (as shown in Figure 4) were 141.7, 216.7, 286.1, 321.7, and 379.6 nm, respectively. Moreover, GeSe nanosheets with different thickness have a huge impact on the experimental results.

The first part of the experiment is the sensing detection of the volume refractive index with five different refractive

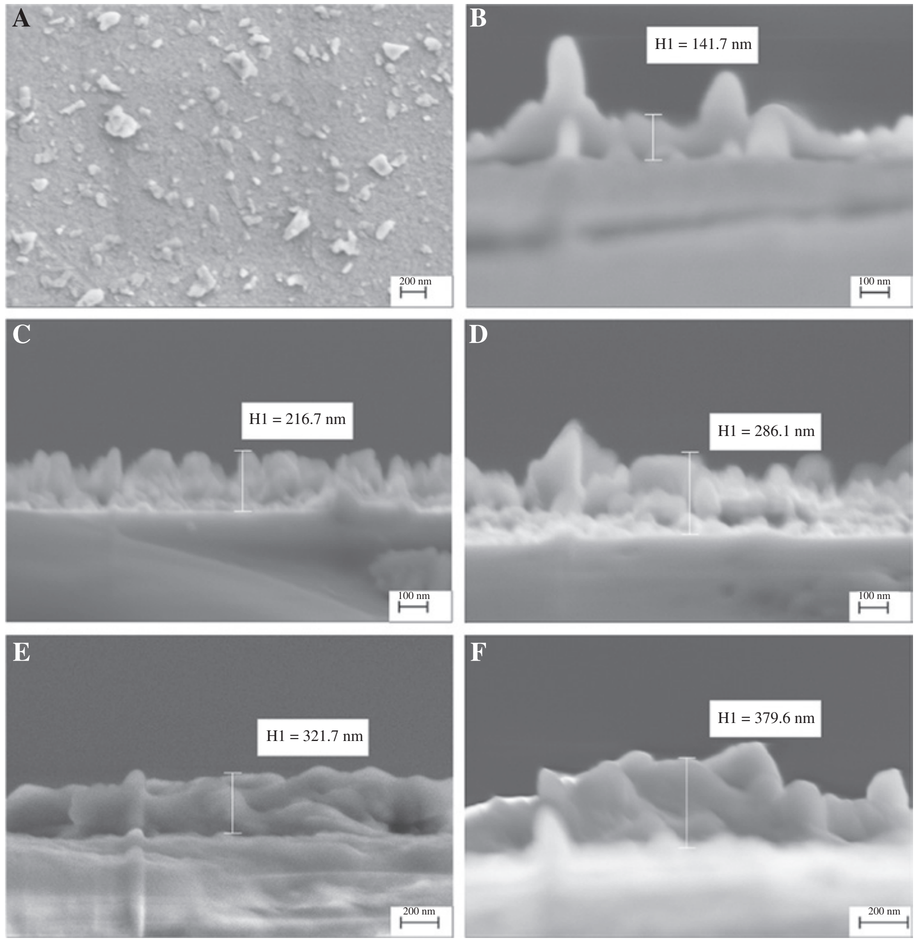

Figure 4: The scanning electron microscope (SEM) image of GeSe nanosheets.
(A) The GeSe surface topography of the presented SPR sensor. SEM images of GeSe nanosheets cross section with different spin coating times for (B) one; (C) two; (D) three; (E) four; (F) five.

index solutions. The reflectance curves of the sensor based on GeSe nanosheets with different thicknesses are shown in Figure 5, where Figure 5A is a reference group containing only gold film. It is obvious that the wavelength position corresponding to the excited resonance peak gradually moves towards the larger wavelength range with the increase of GeSe nanosheets thickness. The maximum peak wavelength shifts at the same changes in refractive index are near 55.8, 73.2, 77.6, 90.9, 100.2, and 71.7 nm for the different spinning times. Therefore, it is demonstrated that the proposed sensor has a high sensitivity in the wavelength-integrated mode due to the larger shifts of peak wavelength. We can estimate that four times coating has the maximum sensitivity. In addition, the minimum reflectance values of the reflection spectrum are gradually increased and the SPR peaks become wider, eventually obtaining a larger value of FWHM.

In order to analyze more intuitively, the SPR sensor sensitivity enhancement relationship based on GeSe nanosheets in a certain refractive index (RI) range, a series of linear fitting curves can be observed in the SPR resonant wavelength shift amount with respect to the RI at different GeSe thickness in Figure 6. It can be found that these linear fitting curves can perfectly represent the moving tendency of the resonance wavelength in a RI region, and the linear correlation coefficients R^2 are 0.9942, 0.9937, 0.9923, 0.9941, 0.9976, and 0.9877 successively, as the numbers of spin coating times increasing from 0 to 5, which reveals that there is a perfect linear relationship between resonance wavelength and RI of the sensing layer. According to the definition of sensitivity $S=\Delta\lambda/\Delta n$, the slope of the linear fitting curve can be known as the sensitivity value when taking different GeSe thickness, in which the sensitivities are 1995.7, 2597.3, 2818.5, 3192.3, 3581.3, and 2677.4 nm/RIU in turn. Therefore, it can be confirmed that the sensor sensitivity first increases and then decreases with increasing the number of GeSe spin coating times.

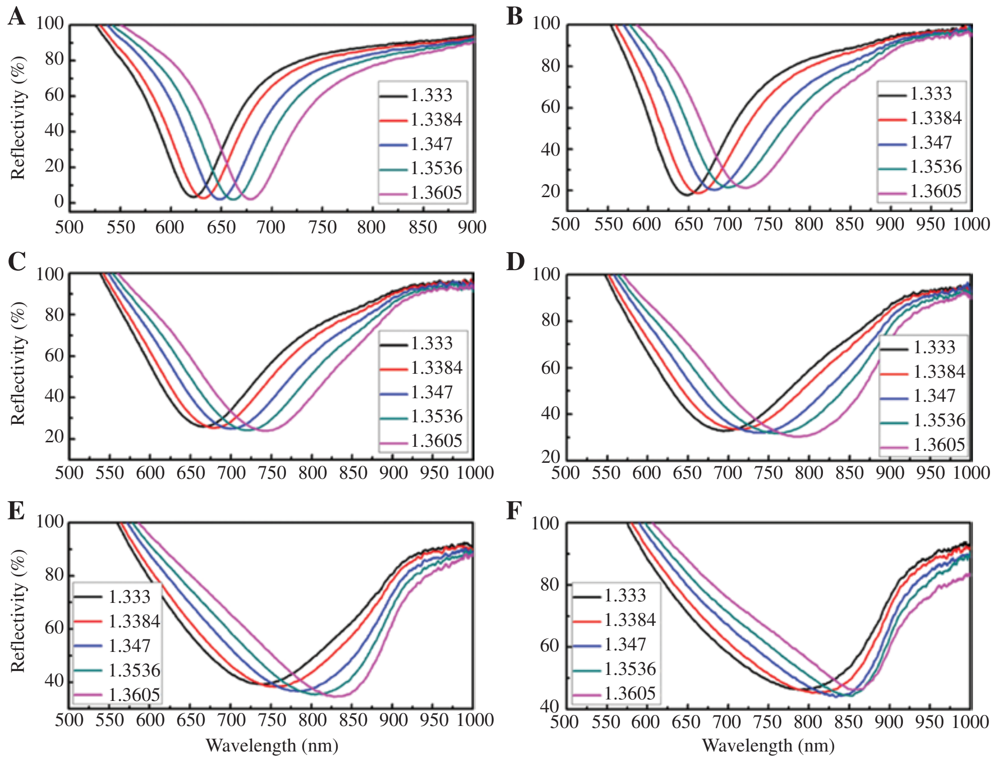

Figure 5: The reflection spectrum of SPR sensor with different thickness GeSe nanosheets.
(A) without spin coating; (B) one; (C) two; (D) three; (E) four; (F) five times spin coating as the refractive index of sensing medium changing from 1.333 to 1.3605.

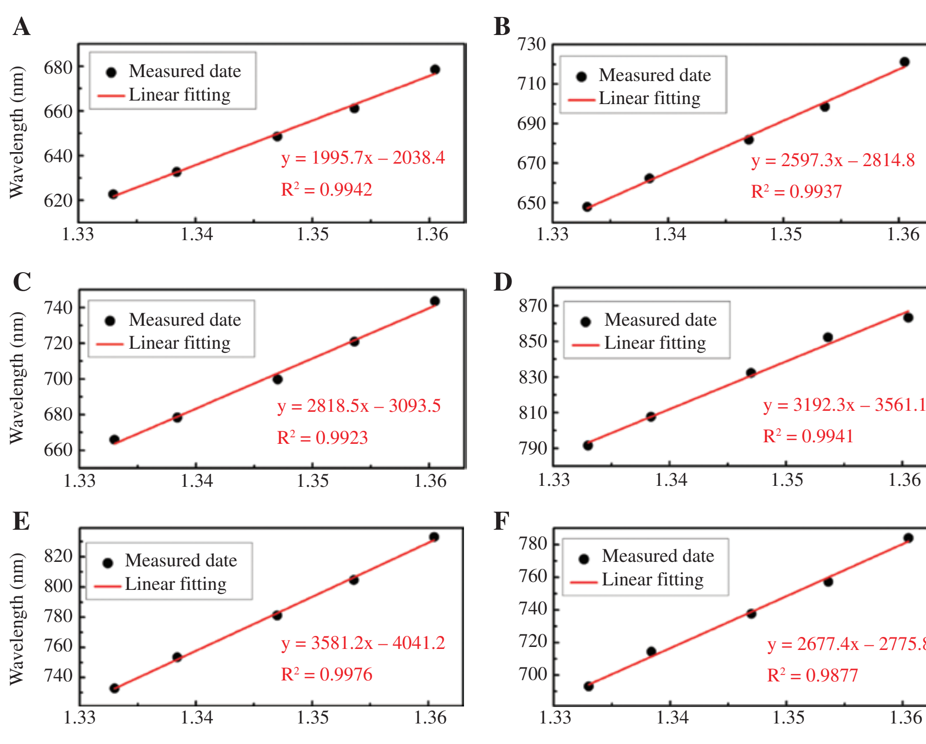

Figure 6: Linear fit curve for the amount of SPR resonant wavelength shift with respect to the refractive index under the condition of different GeSe nanosheets thickness.
(A) without spinning coating; (B) one; (C) two; (D) three; (E) four; (F) five times of spin coating.

As shown in Figure 7A, the maximum enhancement of sensitivity can be achieved as 3581.2 nm/RIU for four times spin coating of GeSe, which is increased by near 80% compared to the control group without spin coating, demonstrating the superior sensitive performance of the proposed sensor. In addition to sensitivity parameters, FWHM and figure of merit (FOM) are also important parameters to reflect sensor quality. Figure 7B,D illustrates the variation of FWHM (at the curve of $n_s=1.333$) and FOM at different GeSe spin coating times from 0 to 5. As the GeSe thickness increases, the resonance gradually broadens, resulting in a larger FWHM value. FOM is usually expressed by the ration of sensitivity to FWHM, which generally shows a large drop under the condition of increasing the times of spin coating.

Next, we applied the GeSe nanosheets modified SPR sensor to detect trace lead ions (Pb^{2+}) due to its excellent sensitivity performance. The time of spin coating with highest sensitivity obtained earlier is selected as the optimal spin coating times for the GeSe and chitosan mixed solution. To completely absorb Pb^{2+} in the detection, it is better to have a full reaction time of 5 to 10 minutes for the sensor chip and heavy metal ions. Figure 8 shows the reflection curves for Pb^{2+} detection with different concentrations ranging from 0 µg/l to 0.8 µg/l by two different SPR sensor structures, namely the Au-chitosan structure and the Au-GeSe-chitosan structure. As shown in Figure 8A, the SPR sensor with only spin-coated chitosan has a small range of resonance wavelength shifts with the increase of Pb^{2+} concentration, which reflects the insufficient sensitivity and the low detection resolution. On the contrary, our proposed SPR sensor with GeSe can detect the small changes of Pb^{2+}concentrations, as shown in Figure 8B. Obviously, with the changes in Pb^{2+} concentration, the measured reflection spectrum becomes wider, and the corresponding resonance wavelength has a larger amount of movement.

Similar to refractive index sensitivity, concentration sensitivity can be defined as $S=\Delta\lambda/\Delta c$, where Δc is the change in concentration of lead ions. Figure 9 has compared the resonance wavelength shifts and sensitivity of two SPR sensors based on Au-chitosan and Au-GeSe-chitosan at different Pb^{2+} concentration changing from 0.20 µg/l to 0.80 µg/l. When Pb^{2+} concentration reaches 0.80 µg/l, the resonance wavelength shifts based on Au-chitosan and Au-GeSe-chitosan SPR sensors are 3.937 nm, and 24.305 nm, respectively, in which the latter is about six times as much as the former. Therefore, the importance of GeSe overlayer for the sensitivity of SPR sensor is verified, and the maximum sensitivity with 30.38 nm/µg/l has been obtained, which is much higher than the conventional SPR sensor covered with chitosan.

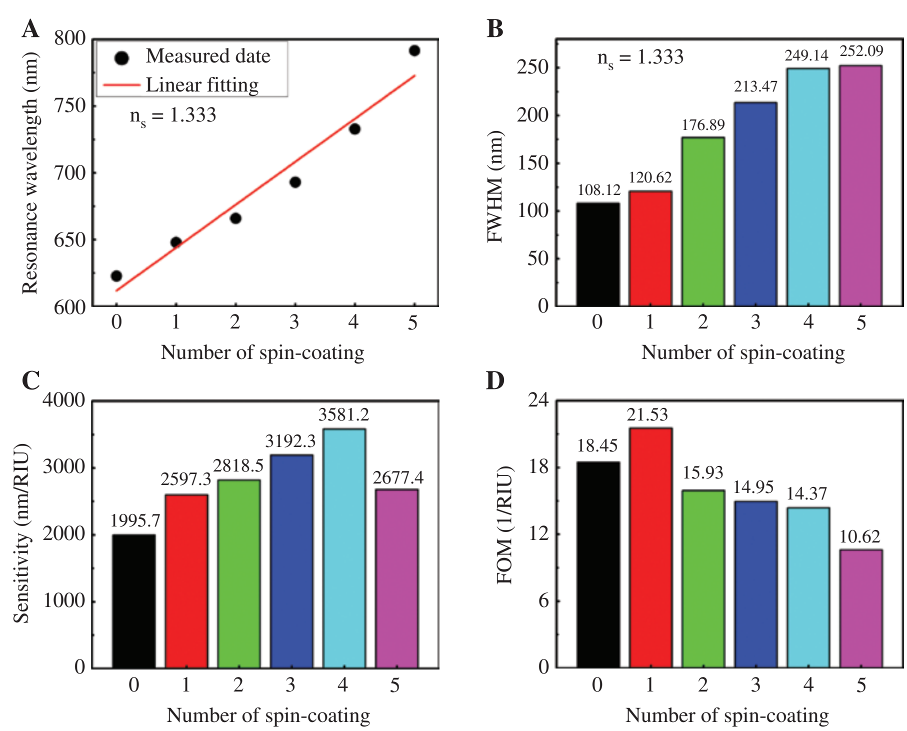

Figure 7: The performances of the presented sensor.
The changes of (A) Resonance wavelength, (B) FWHM, (C) sensitivity and (D) FOM for SPR sensor corresponding to different GeSe spin coating times from 0 to 5.

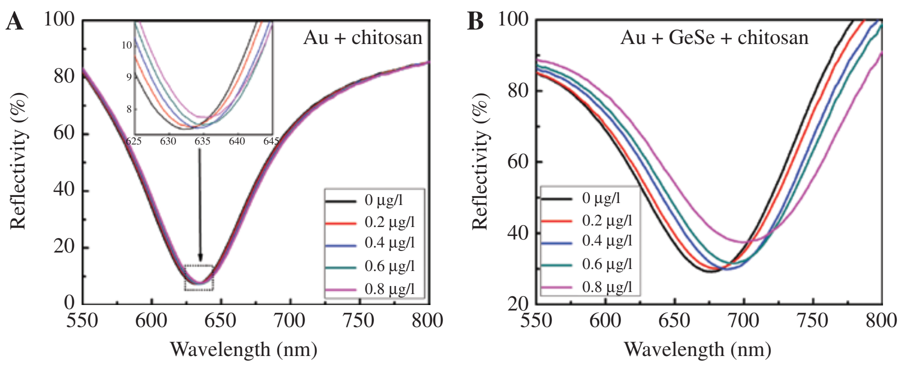

Figure 8: The reflection spectrum of different Pb^{2+} concentrations detection.
The reflection curves about (A) Au-chitosan and (B) Au-GeSe-chitosan based SPR sensor with wavelength interrogation mode under different Pb^{2+} concentrations.

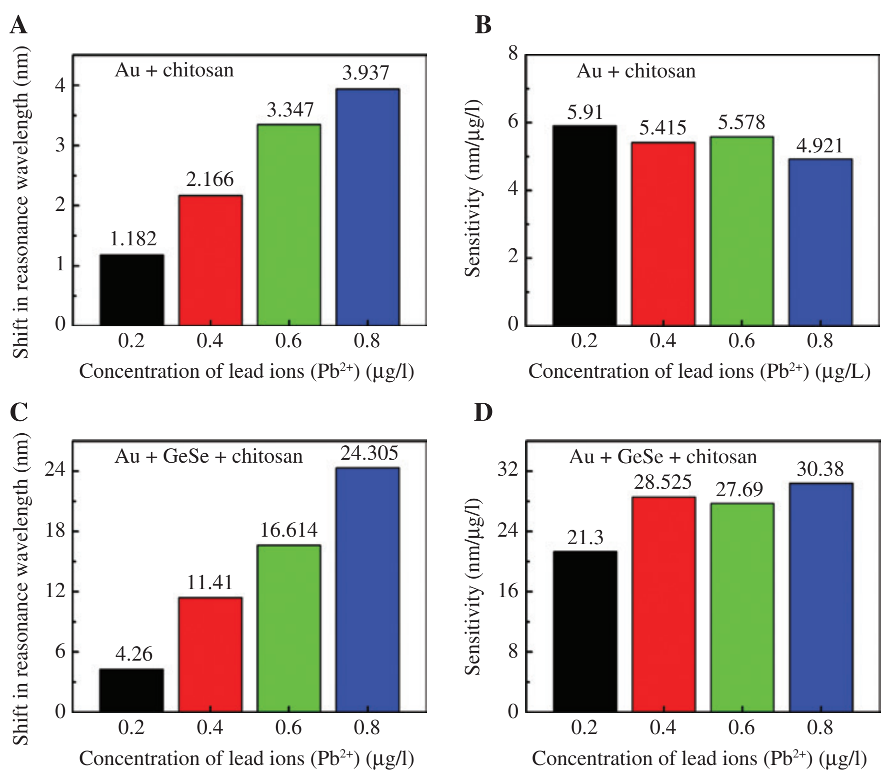

Figure 9: A comparison diagram of sensor performance.
(A) The resonance wavelength shifts and (B) detection sensitivity of the Au-chitosan based sensor with Pb^{2+} concentration changing from 0.20 µg/l to 0.80 µg/l. (C) The resonance wavelength shifts and (D) sensitivity of the Au-GeSe-chitosan based sensor with Pb^{2+} concentration changing from 0.20 µg/l to 0.80 µg/l.

Table 1: Comparison of the latest literatures of the enhancing methods for SPR sensing performance.

Ref.	Enhancement strategy	Analyte	Maximum sensitivity	FOM (1/RIU)
[38]	Au + WS_2	RI solutions	2459.3 nm/RIU	13.23
[39]	Au + MoS_2	RI solutions	2793.5 nm/RIU	11.94
[40]	Au + graphene oxide	RI solutions	2715.1 nm/RIU	19.53
This work	Au + GeSe	RI solutions	3581.2 nm/RIU	14.37
		Pb^{2+} solutions	30.38 nm/µg/l	

Finally, in order to compare with other coatings, we have listed some literatures about wavelength-interrogation SPR sensors based on different coatings, as shown in Table 1, which we observed that the highest sensitivity is achieved in this work.

4 Conclusions

In this study we have proposed a significantly enhanced sensitivity SPR sensor by using GeSe nanosheets. Firstly, the numerical simulation indicates that the GeSe film can enhance the sensitivity significantly. Then we detected five different refractive index solutions, and we illustrated the relativity between the performance of the sensor and the spinning time of 2D materials as well as the increased thickness of GeSe film experimentally. The results showed that the wavelength-interrogation sensitivity can be reached to 3581.2 nm/RIU (nearly 80% improvement compared to traditional SPR sensors) and figure of merit with 14.37 RIU^{-1} for the fourth time spin coating. Moreover, the resonance wavelength has a linear dependent coefficient of 99.76% in detecting the different refractive index of n_s ranging from 1.3330 to 1.3605. Finally, we tried the experiment of sensing Pb^{2+} heavy metals with the proposed sensor, the maximum sensitivity with 30.38 nm/μg/l has been achieved, which is nearly six times better than that the conventional SPR sensor. Our results indicated that SPR sensor modified by GeSe overlayer has the potential in heavy metal detection and chemical-specific molecular identification.

Acknowledgements: This work was partially supported by the National Natural Science Foundation of China (Grant Nos. 61875133 and 11874269, Funder Id: http://dx.doi.org/10.13039/501100001809), the Science and Technology Project of Shenzhen (Grant Nos. JCYJ20180508152903208, CYJ20180305125036005 and JCYJ20180305124842330), the Guangdong Natural Science Foundation (Grant No. 2018A030313198), and the China Postdoctoral Science Foundation (Grant Nos. 2017M622746 and 2018M633129).

Conflicts of interest: There are no conflicts to declare.

References

[1] Yap W, Yang Z, Mehboudi M, Yan J, Barraza-Lopez S, Zhu W. Layered material GeSe and vertical GeSe/MoS2 p-n heterojunctions. Nano Res 2018;11:420–30.
[2] Mishra A, Mishra S, Verma R. Graphene and beyond graphene MoS2: a new window in surface-plasmon-resonance-based fiber optic sensing. J Phys Chem C 2016;120:2893–900.
[3] Wu L, Wang Q, Ruan B, et al. High-performance lossy-mode resonance sensor based on few-layer black phosphorus. J Phys Chem C 2018;122:7368–73.
[4] Xia F, Wang H, Xiao D, Dubey M, Ramasubramaniam A. Two-dimensional material nanophotonics. Nat Photonics 2014;8:899–907.
[5] Wang Y, Ou J, Chrimes A, et al. Plasmon resonance of highly doped two-dimensional MoS2. Nano Lett 2015;15:883–90.
[6] Chockla A, Harris J, Korgel B. Colloidal synthesis of germanium nanorods. Chem Mater 2011;23:1964–70.
[7] Antunez P, Buckley J, Brutchey R. Tin and germanium monochalcogenide IV-VI semiconductor nanocrystals for use in solar cells. Nanoscale 2011;3:2399–411.
[8] Shi G, Kioupakis E. Anisotropic spin transport and strong visible-light absorbance in few-layer SnSe and GeSe. Nano Lett 2015;15:6926–31.
[9] Xue D, Tan J, Hu J, Hu W, Guo Y, Wan L. Anisotropic photoresponse properties of single micrometer-sized GeSe nanosheet. Adv Mater 2012;24:4528–33.
[10] Song X, Zhou W, Liu X, Gu Y, Zhang S. Layer-controlled band alignment, work function and optical properties of few-layer GeSe. Physica B 2017;519:90–4.
[11] Vaughn D, Patel R, Hickner M, Schaak R. Single-crystal colloidal nanosheets of GeS and GeSe. J Am Chem Soc 2010;132:15170–2.
[12] Akimoto T, Sasaki S, Ikebukuro K, Karube I. Effect of incident angle of light on sensitivity and detection limit for layers of antibody with surface plasmon resonance spectroscopy. Biosens Bioelectron 2000;15:355–62.
[13] Shalabney A, Abdulhalim I. Sensitivity-enhancement methods for surface plasmon sensors. Laser Photonics Rev 2011;5:571–606.
[14] Wu L, Chu H, Koh W, Li E. Highly sensitive graphene biosensors based on surface plasmon resonance. Opt Express 2010;18:14395–400.
[15] Hossain M, Bana M. DNA hybridization detection based on resonance frequency readout in graphene on Au SPR biosensor. J Sensors 2016;2016:6060742.
[16] Kretschmann E, Raether H. Radiative decay of non-radiative surface plasmons excited by light. Z Nat 1968;A23:2135–6.
[17] Maurya J, Prajapati Y, Singh V, Saini J, Tripathi R. Performance of graphene-MoS2 based surface plasmon resonance sensor using silicon layer. Opt Quant Electron 2015;47:3599–611.
[18] Rahman M, Anower M, Hasan M, Hossain M, Haque M. Design and numerical analysis of highly sensitive Au-MoS2-graphene based hybrid surface plasmon resonance biosensor. Opt Commun 2017;396:36–43.
[19] Homola J. Present and future of surface plasmon resonance biosensors. Anal Bioanal Chem 2003;377:528–39.
[20] Pounds J, Long G, Rosen J. Cellular and molecular toxicity of lead in bone. Environ Health Perspect 1991;91:17–32.
[21] Dietert R, Lee J, Hussain I, Piepenbrink M. Developmental immunotoxicology of lead. Toxicol Appl Pharmacol 2004;198:86–94.
[22] Hohnadel D, Sunderman F, Nechay M, Mcneely M. Atomic absorption spectrometry of nickel, copper, zinc, and lead in sweat collected from healthy subjects during sauna bathing. Clin Chem 1973;19:1288–92.
[23] Bannon D, Murashchik C, Zapf C, Farfel M, Chisolm J. Graphite furnace atomic absorption spectroscopic measurement

of blood lead in matrix-matched standards. Clin Chem 1994;40:1730–4.
[24] Bannon D, Chisolm J. Graphite furnace atomic absorption spectrophotometry for blood lead analysis. Clin Chem 2001;47:1703–4.
[25] Goossens J, Moens L, Dams R. Inductively coupled plasma mass spectrometric determination of heavy metals in soil and sludge candidate reference materials. Anal Chim Acta 1995;304:307–15.
[26] Manea S, Luca R, Prodana M. Application of inductively coupled plasma-mass spectrometry to investigate the presence of trace metals in human tooth. Eur Cell Mater 2008;16:10.
[27] Chang B, Park S. Electrochemical impedance spectroscopy. Annu Rev Anal Chem 2010;3:207–29.
[28] Fen Y, Yunus W. Utilization of chitosan-based sensor thin films for the detection of lead ion by surface plasmon resonance optical sensor. IEEE Sens J 2013;13:1413–8.
[29] Optical constants of BK7, https://refractiveindex.info/?shelf=glass&book=BK7&page=SCHOTT.
[30] Optical constants of Cr, https://refractiveindex.info/?shelf=main&book=Cr&page=Johnson.
[31] Optical constants of Au, https://refractiveindex.info/?shelf=main&book=Au&page=Johnson.
[32] Liu S, Mi Y, Xue D, et al. Investigation of physical and electronic properties of GeSe for photovoltaic applications[J]. Adv Electron Mater 2017;3:1700141.
[33] Zhao H, Mao Y, Mao X, et al. Band structure and photoelectric characterization of GeSe monolayers. Adv Funct Mater 2018;28:1704855.
[34] Zhan T, Shi X, Dai Y, Liu X, Zi J. Transfer matrix method for optics in graphene layers. J Phys Condens Matter 2013;25: 215301.
[35] Lahav A, Auslende M, Abdulhalim I. Sensitivity enhancement of the guided wave surface-plasmon resonance sensors. Opt Lett 2008;33:2539–41.
[36] Shalabney A, Abdulhalim I. Electromagnetic fields distribution in multilayer thin film structures and the origin of sensitivity enhancement in surface plasmon resonance sensors. Sen Actuators A 2012;159:24–32.
[37] Yang Q, Qin L, Cao G, Zhang C, Li X. Refractive index sensor based on graphene-coated photonic surface-wave resonance. Opt Lett 2018;43:639–2.
[38] Wang H, Zhang H, Dong J, et al. Sensitivity-enhanced surface plasmon resonance sensor utilizing a tungsten disulfide (WS_2) nanosheets overlayer. Photonics Res 2018;6:485–91.
[39] Chen Y, Hu S, Wang H, et al. MoS_2 nanosheets modified surface plasmon resonance sensors for sensitivity enhancement. Adv Opt Mater 2019;7:1900479.
[40] Xiong X, Chen Y, Wang H, et al. Plasmonic interface modified with graphene oxide sheets overlayer for sensitivity enhancement. ACS Appl Mater Interfaces 2018;10:34916–23.